The assembly of microbial communities on red sandstone surfaces was shaped by dispersal limitation and heterogeneous selection

Bowen Wang [a, b], Chengshuai Zhu [a], Xin Wang [c], Tianyu Yang [d], Bingjian Zhang [a, c] and Yulan Hu [a*]

[a] Department of Archaeology, Cultural Heritage and Museology, Zhejiang University, Hangzhou, 310028, China.
[b] Department of Biology, Johns Hopkins University, Baltimore, MD, 21218, USA.
[c] Department of Chemistry, Zhejiang University, Hangzhou, 310028, China.
[d] Leshan Giant Buddha Grottoes Research Institute, Leshan Giant Buddha Scenic Area Management Committee, Leshan, 614000, China.

[*]Corresponding: hu_yulan@zju.edu.cn

Abstract

Understanding the role of microbiota on stone surface is essential for developing effective grottoes conservation strategies. However, ecological feature of microbial communities on stone surface have been rarely investigated systematically. In this study, we explored diversity, assembly, and functional profiles of microbial communities on the red sandstone surface of the Leshan Giant Buddha from microbial ecology perspective. The results show that Proteobacteria, Actinobacteria, Cyanobacteria, and Ascomycota are the dominant phyla. Fundamental metabolic pathways are maintained during the formation of visually distinguishable microbial communities, but gene profiles vary across microbial communities of different colors. Ecological modelling suggests that selective pressure from the harsh stone surface environment fostered the interplay of dispersal limitation and heterogeneous selection during community assembly. The assembly of visually distinct microbial communities is linked to a narrower ecological niche, higher proportion of habitat specialists, elevated complexity, and increased resilience of the prokaryotic network to disturbances. Microbial-mediated ammonium assimilation and nitrogen mineralization might be the two prominent processes that contribute to stone biodeterioration. This study deepens our understanding of the assembly mechanisms and functional potentials of microbial communities on stone cultural heritage surfaces, provides microbial ecological insights for the conservation of these cultural treasures.

Importance: Minimal systematically research on the ecological interpretation of stone biodeterioration. This study reports dispersal limitation and heterogeneous selection shape the microbial community assembly responsible for the biodeterioration of red sandstone. Furthermore, fundamental metabolic processes of microbial communities, such as ammonium assimilation and nitrogen mineralization, are identified as contributors to stone biodeterioration. This study improves our understanding of microbial community assembly and their functional roles, providing a microbial ecological basis for developing effective strategies for the conservation of stone cultural heritage.

Keywords: Community assembly; Microbial community; Microbial diversity; Microbial ecology; Stone; Cultural Heritage

1. Introduction

Grottoes are a common form of stone cultural heritage. The stone surface of grottoes are integral components of ecosystems, providing critical habitats for microbial communities, serving as crucial habitats for microorganisms organized into diverse microbial communities[1-3]. Under specific conditions, these microbial communities can reinforce the stone through metabolic processes like biomineralization[1,4-7]. However, in most cases, the microbial communities on stone surface not only diminish the aesthetic value of the artifacts by obscuring and deteriorating the carvings but may also, in some cases, compromise the structural integrity of the grottoes through severe erosion process[3,8-11]. Therefore, cleaning and controlling the formation of microbial communities on stone surface are essential tasks in the conservation of stone cultural heritage. Understanding the characteristics of microbial communities on stone surface is crucial for developing effective strategies to mitigate microbial deterioration. Currently, research in this field primarily focuses on the taxonomic diversity of microorganisms and their biogeochemical cycling and metabolic capabilities. These studies have revealed the key microbial groups involved in the biodeterioration of stone cultural heritage and their associated biogeochemical processes and metabolic responses[10,12-17]. However, ecological understanding of how microbial communities assemble on the stone surface remains significantly limited.

The ecological mechanisms that govern microbial community assembly are one of the main scientific questions in ecological research[18-20]. It is generally believed that the assembly of local microbial communities is controlled by the combined effects of deterministic and stochastic processes[21-23]. Deterministic processes are used to describe the traditional niche-based theory, which hypothesize that species traits, interspecific interactions, and environmental factors govern community structure[24,25]. In contrast, stochastic processes are based on the neutral theory, which illustrate that community assembly is driven by stochastic events such as birth, death, colonization, extinction, and speciation[26,27]. The niche on the stone surface exposes microorganisms to environmental stresses (abiotic and biotic constraints that limit species productivity and ecosystem development[28]) from nutrient and water scarcity, as well as extreme fluctuations in temperature, humidity, and solar UV radiation[1]. Generally, environmental stress increases deterministic assembly while reducing stochastic assembly, because species with higher tolerance or adaptability to these stressors tend to survive and thrive[28-30]. Furthermore, under high-stress conditions, microbial dispersal limitations are enhanced because elevated stress impedes colonization and successful establishment[28,31,32]. A recent study on microbial communities on limestone surface revealed that prokaryotes and fungi in this environment are primarily dominated by the mutual effect of dispersal limitation (stochastic process) and homogeneous selection (deterministic process)[3]. However, it is currently unknown whether such community assembly mechanisms are specific to certain stone type, geographic location, or

influenced by other factors.

The Leshan Giant Buddha, a world-renowned UNESCO World Heritage site, is a typical example of red sandstone grotto cultural heritage. Previous studies found abundant nitrogen-metabolizing microorganisms and ammonia monooxygenase genes, linked to biodeterioration, on the surface of the Leshan Giant Buddha, which suggests that the deterioration of the stone is closely related to microbial growth[33-35]. The cleaning of stone surface is a crucial task for conservation of the grotto. The current issue is that despite regular cleaning of the stone surface by heritage conservators, visually distinguishable microbial communities persistently reappear after each cleaning. However, our understanding of how microorganisms assemble microbial communities on the stone surface of the Leshan Giant Buddha, as well as on other red sandstone surfaces, remains limited. There is an essential need to investigate the mechanisms by which microbes survive and how they form microbial communities within such ecosystems under various environmental stresses from the perspective of microbial ecology. Therefore, this study uses the Leshan Giant Buddha, a UNESCO World Heritage site, as a case study to provide a comprehensively microbial ecological evaluation to the microbial communities on the surface of this red sandstone cultural heritage. The goal of this study is to examine whether the ecological characteristics of microbial communities on red sandstone surfaces are associated with adaptation to harsh environmental conditions. Specifically, we investigate how these microorganisms assemble into stable communities under repeated wet-dry cycles, nutrient limitations, and UV radiation, and what functional capacities they exhibit. Our focus extends beyond the interactions within the microbiota to include the interactions among microorganisms, environmental factors, and the stone substrate.

2. Results

2.1. Taxonomic composition varies by the color of microbial communities

Samples of three different types of visually distinguishable microbial communities, along with blank samples, were collected from the stone surface of the Leshan Giant Buddha. In general, the total 27 samples were grouped and named according to their respective colors (Bla, black; Gre, green; Whi, white; and CK, blank control) (Fig. 1). We then performed amplicon sequencing of conserved phylogenetic marker genes (16S and ITS rRNA) to identify bacteria and fungi within the microbial communities. After quality filtering and rarefaction, a total of 8,791 and 2,404 non-zero ASVs were obtained from the 16S and ITS sequences, respectively. Each group of data overlap with others, but they are not entirely identical or inclusive of each other (Fig. S1). In addition, metagenome sequencing was applied for each group and obtained 206,491,166 clean reads in total (Table S1).

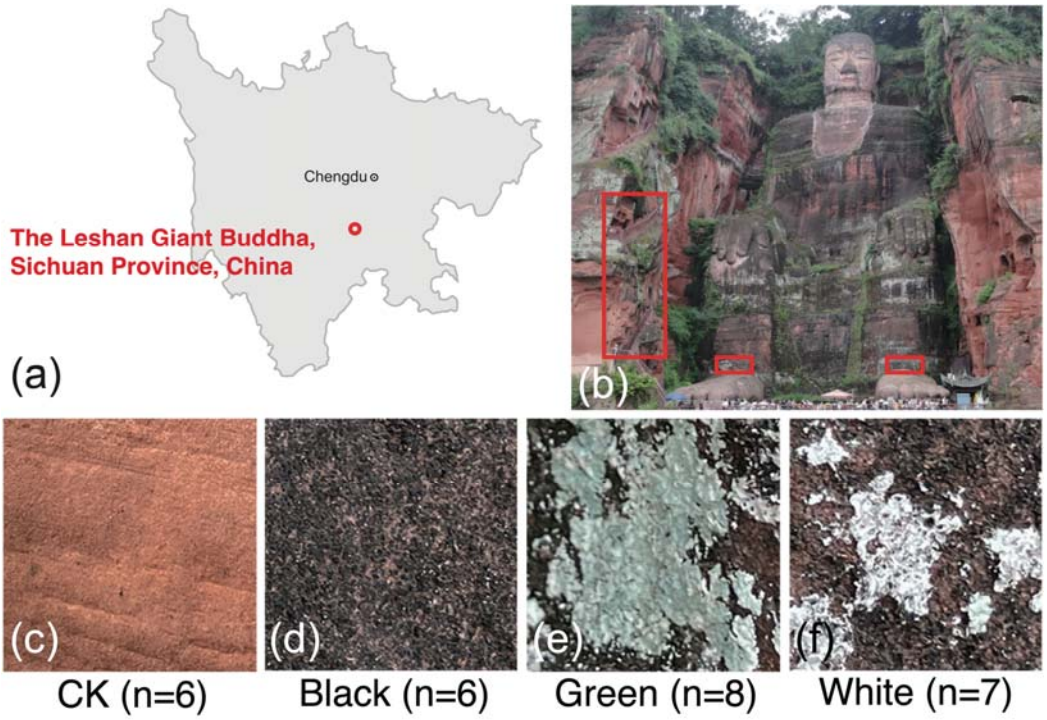

Figure 1. Representative examples and sampling of microbial communities on the red sandstone surface of the Leshan Giant Buddha. (a). Location of the Leshan Giant Buddha. (b). Sampling regions of the samples. Red boxes here indicate the specific sampling regions. (c). Representative examples of CK samples. (d). Representative examples of Black samples. (e). Representative examples of Green samples. (f). Representative examples of White samples. Notes: "n" in picture c-f represents the number of samples used in this study within each group.

To get taxonomic insights into the microbiota, we annotated the sequencing data, then visualized top 10 dominant phyla, top 20 dominant genus of bacteria (Fig. 2 a; Fig. S2 a; Table S2, S3) and fungi (Fig. 2 b; Fig. S2 b; Table S4, S5) among all samples. We also constructed overall taxonomic community composition trees of top 5% dominant bacteria, and top 30% dominant fungi (Fig. 2 c, d). The results show that among all samples, Proteobacteria, Actinobacteria, and Cyanobacteria are the dominant top three phyla in bacteria, comprising at least 70% of the total bacteria in each sample. Ascomycota is the most dominant phylum in fungi, comprising at least 50% of the total fungi in each sample.

To estimate the separation pattern between each group of microbial communities, non-metric multidimensional scaling (NMDS) based on Bray-Curtis dissimilarity at the ASV level was performed and then conducted Anosim (analysis of similarities) and PERMANOVA (*i.e.*, adonis) tests (Fig. 2 e, f). The results show that both bacteria and fungi among the four groups of samples reveal significant and major differences ($P < 0.001$). In summary, the structure of microbial communities varies according to the coloration of the samples, which indicates distinct microbial compositions among samples of different colors.

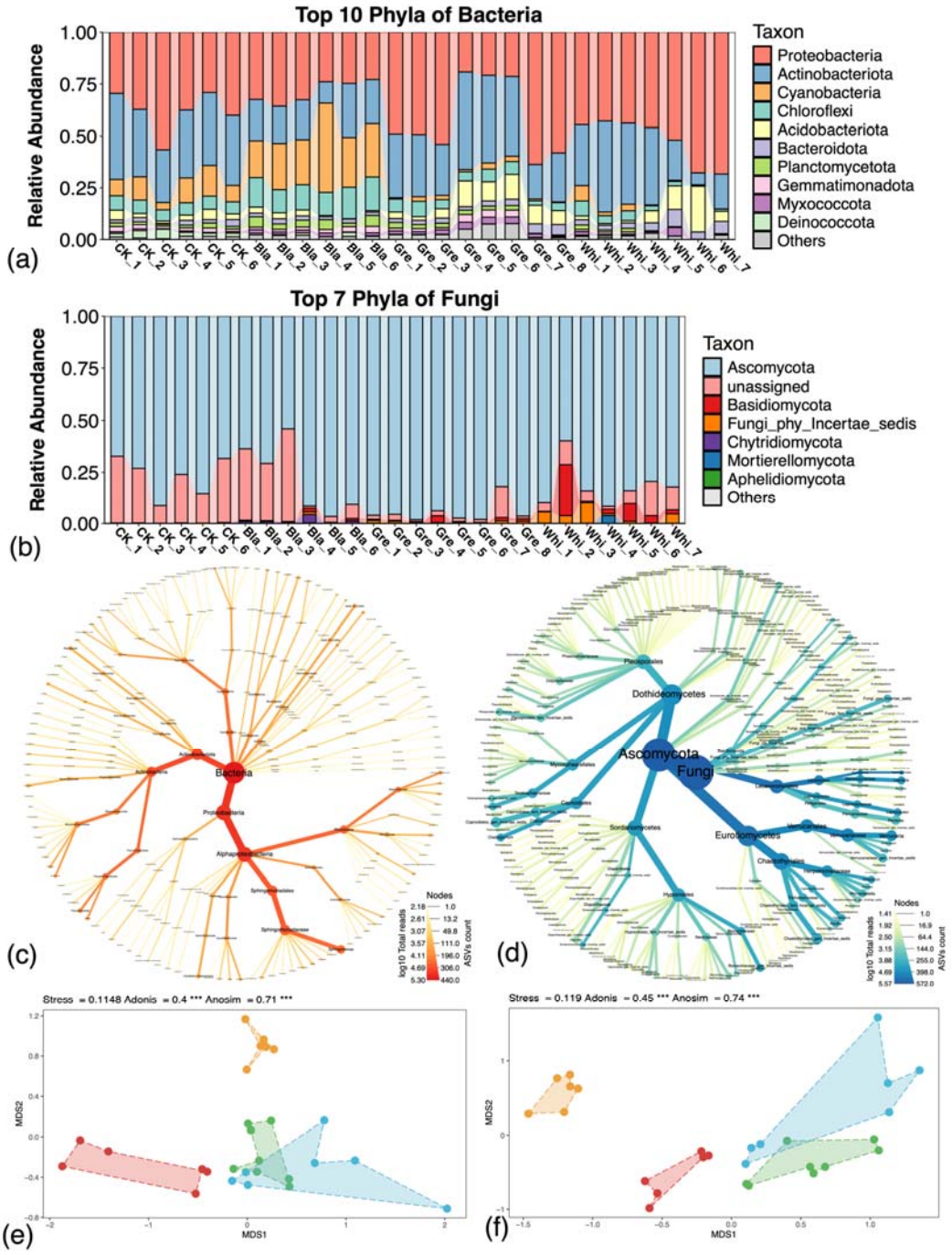

Figure 2. Taxonomic composition and distinct taxonomic structures of the microbial communities. (a). Relative abundances of dominant bacteria among all samples in phylum level. (b). Relative abundances of dominant fungi among all samples in genus level. (c). The overall taxonomic community composition tree of top 5% dominant bacteria. (d). The overall taxonomic community composition tree of top 30% dominant fungi. (e). Non-metric multidimensional scaling (NMDS) ordination based on Bray-Curtis dissimilarities at the ASV level for bacteria. (f). Non-metric multidimensional scaling ordination based on Bray-Curtis dissimilarities at the ASV level for fungi. Notes: The triple asterisks *** represents the $P < 0.001$.

157

158 **2.2. Dispersal limitation and hetero selection dominants the assembly of red sandstone surface**
159 **microbial communities**

160 To characterize the assembly mechanism of the red sandstone surface microbial
161 communities, we applied null model analysis[36,37] and dissimilarity-overlap curve (DOC) model
162 analysis (Fig. 3)[38].

163 Null model analysis showed that both deterministic and stochastic processes controlled the
164 assembly of microbial communities, but the relative importance of the two processes in
165 community assembly vary among sample types (Fig. 3 a, b). In general, dispersal limitation
166 dominated the assembly of both bacteria communities (60.11%) and fungi communities (55.56%)
167 on stone surface. Bacteria revealed overall elevated deterministic process than eukaryotes.
168 Hetero selection and dispersal limitation can explain about 91% of the assembly mechanism of
169 the bacteria communities. While hetero selection and dispersal limitation were also main process
170 for the assembly process of fungi communities; drift played a more pivotal role in the assembly
171 process of fungi communities (20.23%) than in the bacteria ones (5.41%). Bacteria samples
172 revealed significantly higher value of betaNTI than fungi ones (Fig. 3 c). Significant elevation of
173 betaNTI was detected among White groups of bacteria samples comparing with CK (Fig. 3 d). By
174 contrast, significant elevation of betaNTI was detected among Black as well as Green groups of
175 fungi samples comparing with CK (Fig. 3 e).

176 In addition, the DOC model analysis demonstrated a significantly negative correlation
177 between overlap and dissimilarity in both bacteria and fungi communities ($P < 0.001$), which
178 indicated a general dynamic and interspecific interaction within these microbial communities (Fig.
179 3 f, g). These complex dynamic interactions among microorganisms in the microbiota might lead
180 to competition within the shared niche for survival.

181

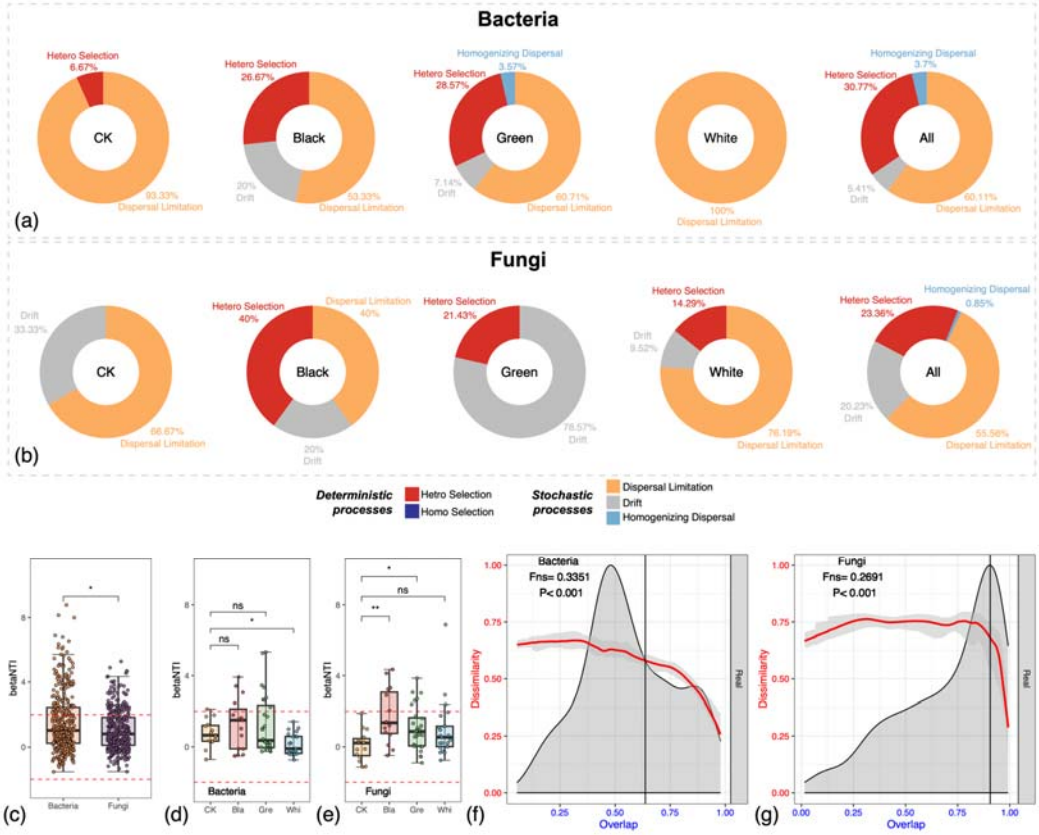

Figure 3. Assembly dynamics of the red sandstone surface microbial communities. (a). The relative importance of assembly processes in bacteria communities. (b). The relative importance of assembly processes in fungi communities. (c). The differences of betaNTI between bacteria and fungi communities. (d). Changes of betaNTI among three groups of bacteria samples comparing with CK. (e). Changes of betaNTI among three groups of fungi samples comparing with CK. (f). Dissimilarity-overlap curve (DOC) analysis of the universality of bacteria dynamics among samples. (g). DOC analysis of the universality of fungi dynamics among samples.

2.3. Specialization prevails over flexibility in microbial community formation on red sandstone surface

To delve deeper into the dynamic interactions among microorganisms within the microbiota, we further investigated the niche characterization of microbial communities on red sandstone surface. According to Levins niche breadth theory, the distribution of microbiota composition can be used as an indicator of the environmental conditions[39]. Here, we calculated niche breadth (*Bcom*) and niche overlap (*Ocom*) as indicators to describe the habitat niche characterization of both bacteria and fungi making up the stone surface microbial communities. First, the *Bcom* was calculated with Levins index (Fig. 4 a-c). The results showed that the visually distinguishable microbial communities revealed decreased overall *Bcom* comparing with CK group. Such results were also further validated with Shannon index (Fig. S3 a-c). Then, the *Ocom* was calculated with Schoener index. The *Ocom* for both bacteria and fungi displayed a similar trend that CK samples revealed the highest *Ocom*, followed by Black, Green, and White, in descending order. All

205 pairwise comparisons were statistically significant, indicating distinct niche overlaps among the
206 different samples. When comparing *Ocom* across all samples, bacteria revealed a significantly
207 higher *Ocom* than fungi (Fig. 4 d-f). Such results were also further validated with Pianka index
208 (Fig. S3 d-f). In summary, both bacteria and fungi communities exhibit significant variations in
209 *Bcom* and *Ocom* across different sample types (CK, Black, Green, White). In general, CK samples
210 displayed widest niche breadth and highest overlap level compared with the rest groups of
211 samples. These results suggested that the formation of visually distinguishable microbial
212 communities on stone surface requires species to be more specialized, rather than relying on
213 diverse and flexible species with metabolic flexibility and redundancy.
214 To further explore the inference, we also calculated the proportion of generalists and
215 specialists among the microbial communities (Fig. 4 g-k). Generalists are species that are better
216 suited to survive in diverse and challenging environments and often play pivotal roles within
217 their communities. Specialists, on the other hand, have a more limited range of habitats and are
218 specifically adapted to environmental conditions[40,41]. The results showed that at the ASVs level,
219 the proportion of specialists in each type of sample was higher than that of generalists in both
220 bacteria and fungi (Fig. 4 g). To determine whether there were differences between all bacteria
221 and fungi, we also compared the proportion of specialists and generalists within these groups.
222 The results showed that in each group of both bacteria and fungi, the proportion of specialists
223 was higher than that of generalists. But, bacteria revealed overall higher proportion of
224 generalists than that of specialists (Fig. 4 g). At the phylum level, up to 69.61 % of the bacteria
225 were classified as the middle; the proportion of specialists (29.95 %) was higher than that of
226 generalists (0.44 %) (Fig. 4 i, Table S6). Myxococcota revealed the largest fraction of specialists in
227 bacteria (52.4%) among the top 10 dominant phyla. (Fig. 4 h, Table S6). For the fungi, 59.5% were
228 classified as middle, 40.5% as specialists, and none of the ASV is classified as generalists. (Fig. 4 k,
229 Table S7). This suggested that specialists prevail over generalists in the dominant phyla within
230 the assembly of microbial communities. Notably, the non-dominant phyla (others) of both
231 bacteria and fungi exhibited the highest proportion of specialists (Fig. 4 h, j; Table S6, S7). This
232 suggested that the non-dominant phyla within the community might have even lower metabolic
233 flexibility compared to the dominant phyla.
234

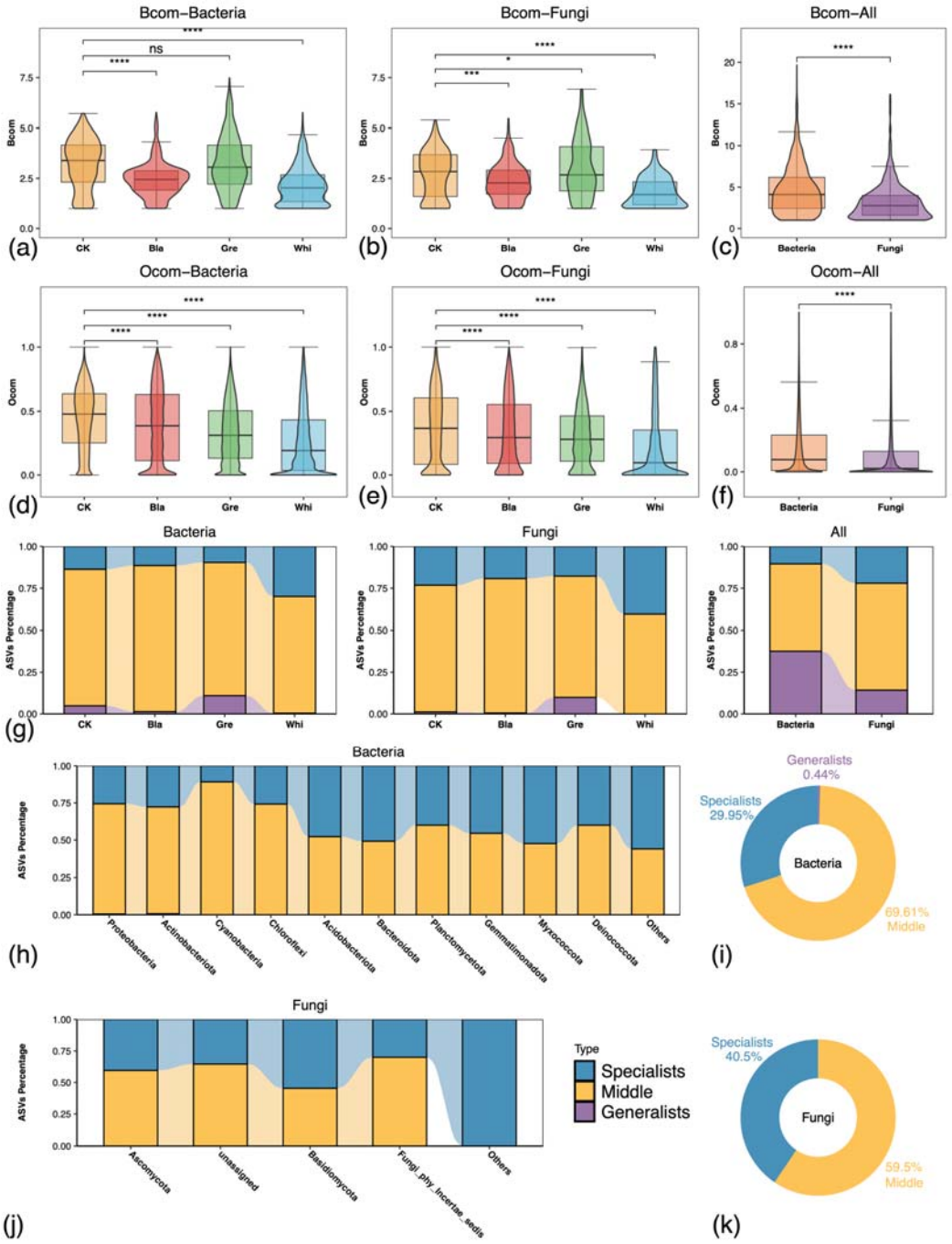

Figure 4. Niche characterization of the red sandstone surface microbial communities based on Levins niche breadth index and Schoener niche overlap index. (a). Average habitat niche breadth (*Bcom*) differences among three groups of bacteria samples comparing with CK in bacteria. (b). *Bcom* differences among three groups of fungi samples comparing with CK in fungi. (c). *Bcom* differences between bacteria and fungi. (d). Average habitat niche breadth (*Ocom*) differences among three groups of bacteria samples comparing with CK in bacteria. (e). Average *Ocom* differences among three groups of fungi samples comparing with CK in fungi. (f). Average *Ocom* differences between bacteria and fungi. (g). Proportional distribution of specialists, middle, and generalists in each sample group, and between bacteria and fungi. (h). Proportional distribution

of specialists, middle, and generalists of bacteria at phylum level based on Levins niche breadth index. (i). Overall proportion of the habitat niche breadth of bacteria at phylum level. (j). Proportional distribution of specialists, middle, and generalists of fungi at phylum level. (k). Overall proportion of the habitat niche breadth of fungi at phylum level. Notes: The *Bocm* was calculated with Levins index. The *Ocom* was calculated with Schoener index. All ASVs were defined as specialists, middle or generalists according to Levins niche breadth index. The asterisks in the boxplots stand for the significance of the Wilcoxon signed-rank test. The "ns" stands for no significance, single asterisk stands for $P < 0.05$, double asterisks stand for $P < 0.01$, Triple asterisks stand for $P < 0.001$, Four asterisks stand for $P < 0.0001$.

2.4. Elevated network complexity and resilience to disturbances during the formation of visually distinguishable microbial communities on red sandstone surface

Given the non-random assembly patterns observed in red sandstone surface microbial communities, we proceeded to construct microbial co-occurrence networks of both bacteria and fungi in different types of microbial communities to further explore the interaction patterns within these communities (Fig. 5).

Topological features analysis of the networks revealed that bacteria network showed higher links (Fig. 5 a). This indicated that the elevation of the complexity of the bacteria network was necessary for the formation of visually distinguishable microbial communities. To evaluate the resilience of the bacteria network to disturbances, we also analyzed the robustness of the network with different approaches including targeted and randomly removal of key species, removal of nodes, as well as the calculation of negative correlation ratio. The results showed that the bacteria network robustness decreased as both targeted and randomly removal of the key species, with Black, Green, and White groups showing greater vulnerability compared to CK (Fig. 5 b, c). The bacteria networks of the three visually distinguishable microbial communities also revealed greater vulnerability to the removal of nodes than CK (Fig. 5 d). In addition, the CK network also revealed higher negative correlation ratio than the Black and White networks of visually distinguishable microbial communities (Fig. 5 e). This implied the formation of the two visually distinguishable microbial communities could mitigate the mutual exclusion of microbial populations in resource competition.

By contrast, the topological features of fungi networks were different from those of bacteria networks. The number of links in the fungi Green group decreased to half compared to the CK group, while the number of links in the White group increased by approximately half (Fig. 5 f). The network robustness analysis results indicated that only the White group demonstrated higher stability across all test categories (Fig. 5 g-j). This suggests that the role of fungi in community formation might be more complex and variable depending on the morphology of communities.

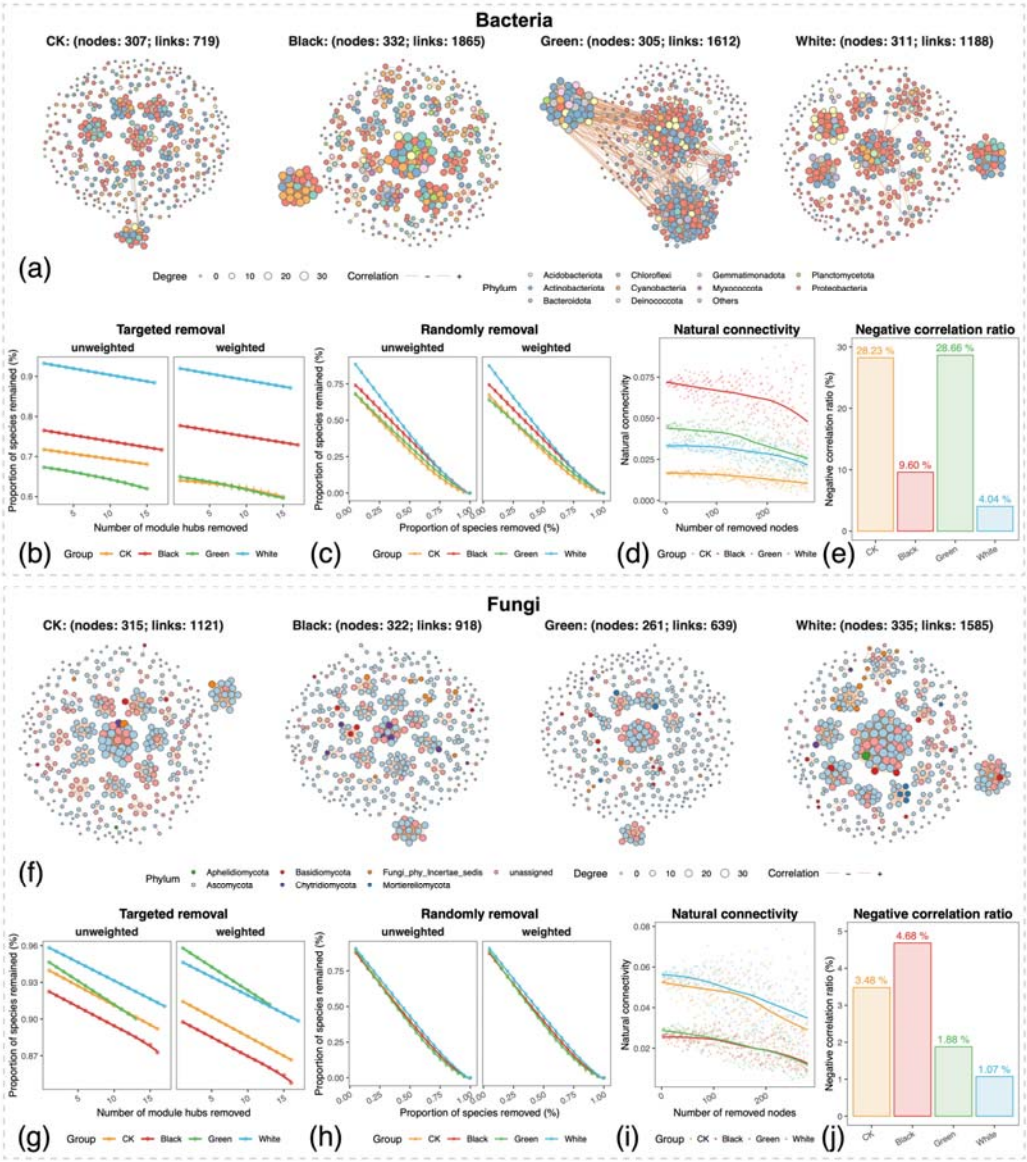

Figure 5. Topological features of the co-occurrence network within microbial communities on the stone surface. (a). Co-occurrence network of bacteria communities. (b). Robustness of bacteria networks under targeted removal of key species. (c). Robustness of bacteria networks under random removal of key species. (d). Vulnerability of bacteria networks under removal of key node. (e). Negative correlation ratio of the bacteria co-occurrence networks within each group. (f). Co-occurrence network of fungi communities. (g). Robustness of fungi networks under targeted removal of key species. (h). Robustness of fungi networks under random removal of key species. (i). Vulnerability of fungi networks under removal of key node. (j). Negative correlation ratio of the fungi co-occurrence networks within each group.

298 **2.5. Fundamental metabolic pathways are maintained but gene profiles vary**

299 To elucidate the metabolic processes that enable the survival of microbial communities on
300 the stone surface, we performed metagenomic sequencing for each type of microbial
301 communities. Ten Gene Ontology (GO) terms that could potentially contribute to the assembly of
302 microbial communities on red sandstone surface were identified in all four types of microbial
303 communities[3]. These terms were associated with functions related to organism interactions,
304 microbial survival, and trophic processes. Each of the ten GO terms was detectable in every
305 group (Fig. 6 a). Next, we used PICRUSt2 to predict the functional potential of the bacterial
306 communities. The results showed significant differences in both enzyme functions (ECs) and
307 metabolic pathway genes (KOs) among the groups (PERMANOVA, $P < 0.05$) (Fig. 6 b, Fig. S4,
308 Table S8, S9), suggesting that the microbial communities in each group adapted to their specific
309 environmental conditions through distinct metabolic details.

310 Nitrogen cycle processes have been broadly reported as closely related with the
311 deterioration of stone[3,9,42-44]. Hence, we performed detailed insight into nitrogen cycle processes.
312 The results showed that relative gene abundance of each nitrogen cycle pathway was consistent
313 across all four types of microbial communities (Fig. S5). Ammonium assimilation and nitrogen
314 mineralization were the two dominant processes among the nitrogen cycle. The two processes
315 possessed accounted for up to 38.52% and 31.39% of the overall abundance of reads within the
316 nitrogen cycle pathways, respectively, which imply the intensive nitrogen-exchanging
317 interactions between microbial communities and the stone surface substrate. Nevertheless, the
318 specific high-abundance genes involved in major nitrogen cycling processes differed across
319 groups, indicating that each group harbors distinct metabolic features within individual nitrogen
320 cycling pathways (Fig. 6 c).

321

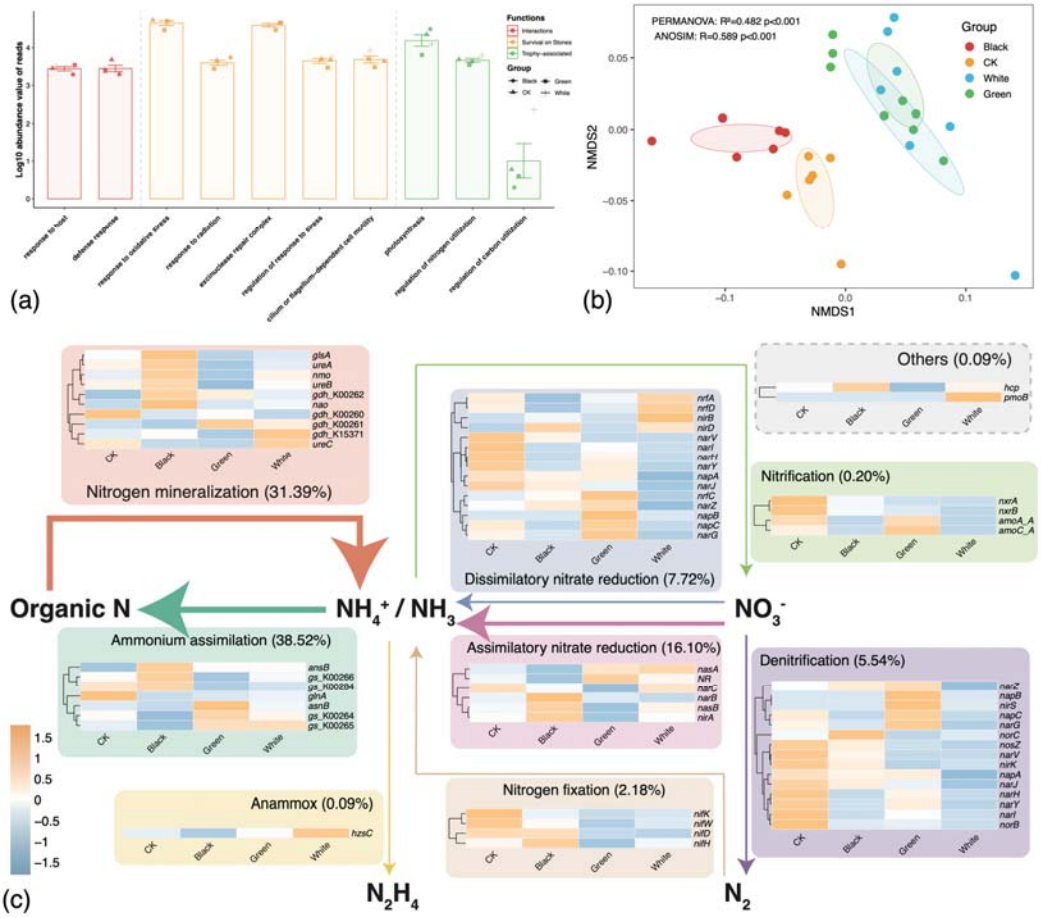

Figure 6. Functional profiles of the stone surface microbiota. (a). GO functional annotation of the stone surface microbiota. (b). Significant differences of enzyme functions (ECs) among four groups. (c). Nitrogen cycling potential of the stone surface microbiota. Arrow thickness corresponds to the proportion of functional genes for corresponding metabolic processes.

3. Discussion

Uncovering the diversity, assembly mechanisms, and functional traits of microbial communities is a central focus in microbial ecology[18,45,46]. Recently, the role of microbial communities on stone surface has garnered increasing attention, particularly in the field of stone cultural heritage conservation[47]. In this study, we present a pioneering case study on the ecological roles of microbiota on red sandstone surface, using the Leshan Giant Buddha as an example. The results indicate that the taxonomic composition of microbial communities varies according to their coloration. During the formation of visually distinguishable microbial communities, core metabolic pathways of microbial communities are maintained but gene profiles vary across different types of microbial communities, particularly in nitrogen cycle-related biogeochemical processes. Dispersal limitation and heterogeneous selection dominate the assembly of stone surface microbial communities. Habitat specialists play a more significant role than generalists during the formation of microbial communities on the red sandstone surface. As visible microbial communities form on stone surface, network complexity

increases, and resistance to disturbances is enhanced. By comparing our findings with previous studies on microbial communities on stone surface, we inferred the following commonalities and unique characteristics in the ecological features of stone surface microbial communities.

3.1. Harsh living conditions on the stone surface might induced conserved core ecological functions of stone surface microbes

In this study, the microbial diversity analysis revealed that Proteobacteria, Actinobacteria, Cyanobacteria, Chloroflexi, and Acidobacteriota dominate the top phyla among the prokaryotes in all samples, while Ascomycota stands as the most dominant phylum in eukaryotes, despite the distinct microbial community morphology across different sample groups. Such phylum-level diversity patterns are largely consistent with previous reports on taxonomic diversity of microbial communities on the surface of other stone types. However, significant differences were observed at the genus level[2-4,34,48-50]. These variations might be attributed to site-specific factors, including the local climate and the types of stone cultural heritage[51]. Comparison with previous studies suggests that core ecological functions of stone surface microbes are conserved across the surfaces of various types of stone. The capability to withstand pressures such as fluctuations between wet and dry conditions, endure UV stress on stone surface, and facilitate ion exchange with the stone appears essential for the persistence of microbial communities on the outdoor stone surface[3,9].

Nitrogen cycle is a crucial way of ion exchange between microbial communities and the stone substrate. In previous study, the two dominated types of nitrogen cycling genes in limestone surface microbial communities are nitrogen assimilation and mineralization, which is coherent with what we found in red sandstone surface microbial communities in this study[3]. Nitrifying bacteria genera *Nitrospira* and *Nitrosomonas* were significantly enriched in limestone surface microbial communities[3]. In another case study involving regular sandstone, *Nitrosopumilus* and *Nitrospira* were also identified from deteriorated sediments[9]. Furthermore, *Methylobacterium*, another dominant genus identified in our study, comprises species recognized as plant growth-promoting rhizobacteria, with genomes encoding enzymes involved in nitrogen metabolism and ammonia assimilation[52]. Notably, in previous study, the two dominated types of nitrogen cycling genes in limestone surface microbial communities are nitrogen assimilation and mineralization, which is coherent with what we found in red sandstone surface microbial communities in this study[3]. Despite this, nitrogen metabolic genes are diverse across different groups, which suggests that members of each type of group microbial community could adapted to the rock surface niche through distinct metabolic details[53].

Conserved core functions among microbial communities within similar niches is not unique to microbial communities on stone surface. For example, several gut microbiota studies have reported functional, but not compositional, convergence of gut microbiomes[54-57]. Some soil microbiota studies also reported the stable functional structure despite high taxonomic variability[58-60]. In addition, microbial functional genes of ocean microbiota that execute certain functions, such as B_{12} biosynthesis, are widely distributed, while the microbial taxa that carry these genes vary significantly[61]. These results corroborate the ecological hypothesis that environment truly selects for function, rather than taxonomy[62]. Different taxonomic groups could reveal convergent functions as a result of functional redundancy among microbial systems[63]. On stone surface, conserved core functions among various types of stones might be attributed to the

386 selective pressure imposed by the harsh living conditions on the stone surface, favoring the
387 survival of microbial communities with specific functions[58,64-66].
388
389 **3.2. Assembly of stone surface microbial communities requires a general pattern of dynamic**
390 **interactions**
391 In this study, we witnessed the extensive microbe-microbe and microbe-environment
392 interactions within the microbial communities on the stone surface. The mutual effect of hetero
393 selection and dispersal limitation controls the assembly process of both prokaryotic and
394 eukaryotic communities on red sandstone surface. Such results differ from previous studies on
395 the assembly process of microbial communities on limestone surface, where the assembly
396 process is driven by hetero selection and dispersal limitation[3]. This suggests that the assembly
397 mechanisms of microbial communities on stone surface might vary based on stone types,
398 geographical locations, climatic characteristics, or other environmental factors. In addition, the
399 results of the DOC model analysis suggest a general pattern of dynamic interspecific interactions
400 within the communities on the red sandstone surface and high selective pressure on the red
401 sandstone surface[38,67-69]. Such complexity was further testified in this study by the topological
402 feature analysis of the microbial networks. The active biogeochemical metabolism such as
403 ammonium assimilation and nitrogen mineralization processes by the microbial communities also
404 suggests their active interactions with the red sandstone substrate[70]. The elevated complexity of
405 microbial communities might arise from widely functional complementarity and the resulting
406 extensive interactions among microbes[71].
407 Here, we propose a hypothesis that a possible model capable of precisely interpreting the
408 assembly processes of stone surface microbial communities is the classic MacArthur
409 consumer-resource model, where species-species interactions are mediated through resource
410 dynamics[72-74]. Because the nutrient-poor nature of stone surface, the colonization by pioneer
411 species is primarily driven by deterministic processes linked to nutrient availability, which aligns
412 with commonly observed among natural communities from various locations[75]. Some pioneer
413 species utilize inorganic energy from the stone to establish themselves. These species then leak
414 metabolic by-products into the environment, increasing the diversity of resources and enhancing
415 the biocompatibility of the stone surface. Other species can subsequently utilize these leaked
416 metabolites, in turn releasing new by-products into the environment, further enhancing the
417 biocompatibility of the stone surface, and facilitating the formation of microbial communities.
418 The observed decrease in ecological niche breadth among the visually distinguishable microbial
419 communities in this study also suggests that the utilization of specific resources is more efficient
420 within these communities. We also observed that specialization prevails over flexibility during
421 the formation of microbial communities on red sandstone surface. This is consistent with a
422 previous study on the assembly of microbial communities in a wide range of well-defined
423 resource environments, where habitat specialists also drive the increase of diversity in such
424 microbial communities[19].
425
426 **3.3. Summary**
427 In summary, this study focuses on microbial communities on the surface of red sandstones
428 of the Leshan Giant Buddha, which reveals their ecological and functional characteristics. Under
429 the interplay of dispersal limitation and hetero selection, the microbiota on the red sandstone

were assembles into distinct types of visually distinguishable microbial communities., significantly differentiate the taxonomic composition of these communities. However, under the harsh habitant on red sandstone surface, such as UV radiation, fluctuations between dry and wet conditions, and limited nutrient availability, the core functions of the microbe among different types of microbial communities are convergent. These functions are particularly enriched in biogeochemical processes related to nitrogen cycling and responses to environmental stress. The formation of visually distinguishable microbial communities is associated with a narrower niche width, elevated complexity, and increased resilience of the prokaryotic network to disturbances. Furthermore, a higher proportion of habitat specialists are found in microbes forming these visually distinguishable microbial communities (Fig. 7). Given the nutrient limitations of the red sandstone surface, the classic MacArthur consumer-resource model might provide a potential framework to further explain the assembly mechanisms of these microbial communities. Future research into the ecological traits and functional potential of these microbial communities will provide critical insights for managing microbial communities on red sandstone surface. Moreover, microbial deterioration affects not only stone cultural heritage but also a wide range of different cultural heritage materials[76-80]. The microbial ecology-based approach used in this study will help advance research on microbial deterioration mechanisms in other cultural heritage materials, providing a model for future work.

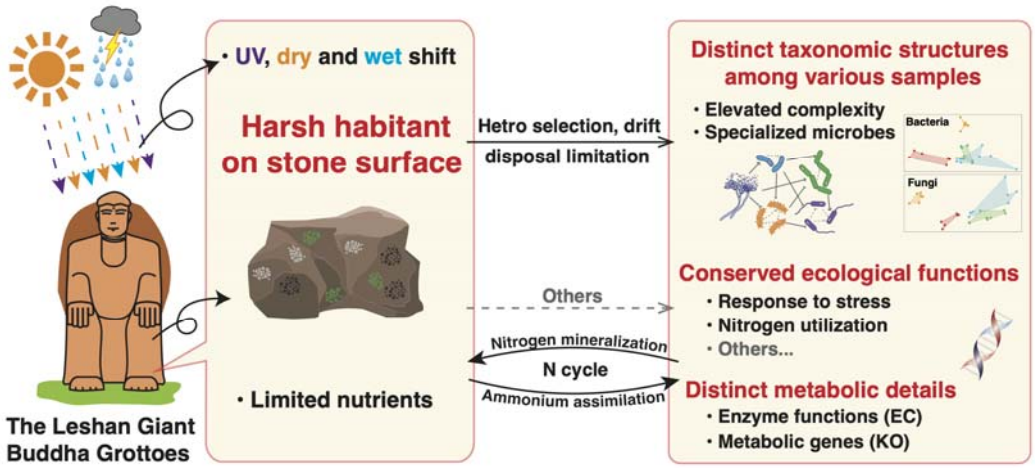

Figure 7. Schematic diagram illustrates the characteristics of microbial communities on the red sandstone surface of the Leshan Giant Buddha

4. Materials and Methods

4.1. Sampling processes

The Leshan Giant Buddha is a world-famous, typical red sandstone-made, UNESCO World Heritage site. It was built between 713 and 803 during the Tang dynasty, located in the Leshan city, Sichuan province, China. Samples used in this study were collected from the stone surface of the Leshan Giant Buddha between 2019 and 2022. Among these, 6 samples have been used in our previous study[34]. The other 21 samples were newly collected in 2022. Surface samples were scraped using a pre-cleaned steel scalpel and then stored in low temperature until DNA

extraction.

4.2. DNA extraction and NGS sequencing

The DNA extraction was applied using a genomic DNA extraction kit from TIANGEN (DP302-02) with 0.5 g of sample processed for extraction. The amplicon sequencing was performed as followed. The 16S V3-V4 region rDNA and ITS2 region were amplified by PCR (initial denaturation at 98 ℃ for 30 seconds; 32cycles of denaturation at 98 ℃ for 10 seconds, annealing at 54℃ for 30 seconds, and extension at 72 ℃ for 45 seconds; and then final extension at 72 ℃ for 10 minutes.) with following primers: 0341-F (CCT ACG GGN GGC WGC AG) and 806-R (GAC TAC HVG GGT ATC TAA TCC) for 16S[81], ITS1FI2 (GTG ART CAT CGA ATC TTT G) and ITS2 (TCC TCC GCT TAT TGA TAT GC) for ITS2. The PCR products were purified by AMPure XT beads (Beckman Coulter Genomics, Danvers, MA, USA) and quantified by Qubit (Invitrogen, USA). The amplicon pools were prepared for sequencing and the size and quantity of the amplicon library were assessed on Agilent 2100 Bioanalyzer (Agilent, USA) and with the Library Quantification Kit for Illumina (Kapa Biosciences, Woburn, MA, USA), respectively, and then sequenced on Illumina NovaSeq 6000 PE250 platform in LC-Bio Technology Co., Ltd, Hang Zhou, Zhejiang Province, China. The raw sequence data were then deposited in the Genome Sequence Archive[82] in National Genomics Data Center[83], China National Center for Bioinformation / Beijing Institute of Genomics, Chinese Academy of Sciences (GSA: CRA013382) that are publicly accessible at https://ngdc.cncb.ac.cn/gsa.

The DNA libraries were sequenced on the illumina NovaseqTM 6000 platform by LC Bio Technology CO., Ltd (Hangzhou, China). We are grateful to LC Bio Technology CO., Ltd for assisting in sequencing. DNA concentration was measured using Qubit. Based on the measured concentration, equal-mass DNA samples were pooled from all samples within each group by mixing 100 ng of DNA from each sample. The metagenome sequencing was performed as followed: DNA library was constructed by TruSeq Nano DNA LT Library Preparation Kit (FC-121-4001). DNA was fragmented by dsDNA Fragmentase (NEB, M0348S) by incubate at 37°C for 30min. Library construction begins with fragmented cDNA. Blunt-end DNA fragments are generated using a combination of fill-in reactions and exonuclease activity, and size selection is performed with provided sample purification beads. An A-base is then added to the blunt ends of each strand, preparing them for ligation to the indexed adapters. Each adapter contains a T-base overhang for ligating the adapter to the A-tailed fragmented DNA. These adapters contain the full complement of sequencing primer hybridization sites for single, paired-end, and indexed reads. Single- or dual- index adapters are ligated to the fragments and the ligated products are amplified with PCR. The raw sequence data were then deposited in the Genome Sequence Archive[82] in National Genomics Data Center[83], China National Center for Bioinformation / Beijing Institute of Genomics, Chinese Academy of Sciences (GSA: CRA013393) that are publicly accessible at https://ngdc.cncb.ac.cn/gsa.

4.3. Taxonomic and functional annotations

For the amplicon sequencing data, the DADA2 R package[84] in QIIME 2[85] was used to conduct a complete pipeline to generate raw paired-end fastq sequencing files into merged, denoised, chimera-free sequences and output ASV. The ASV tables for both 16S and ITS were rarified to a minimum sequencing depth (13,622 for 16S and 16,232 for ITS) to mitigate the impact of

505 sequencing depth on subsequent analysis. Representative ASV sequences were classified into
506 different organisms using a naive Bayesian model with RDP classifier[86], which is based on the
507 SILVA database[87] (version 138) for 16S or UNITE database[88] (version 9.0) for ITS.
508 Metagenome raw sequencing reads were processed to obtain valid reads for further analysis.
509 First, sequencing adapters were removed from sequencing reads using cutadapt (version 1.9).
510 Secondly, low quality reads were trimmed by fqtrim (version 0.94) using a sliding-window
511 algorithm. Window size is 6 bp, and base quality must not be lower than 20. Once quality-filtered
512 reads were obtained, they were de novo assembled to construct the metagenome for each
513 sample by MEGAHIT with the following parameters: *--k-list 21,29,39,59,79,99,119,141 -m 0.8 -t 8*
514 *--min-contig-len 200 --continue*. All coding regions (CDS) of metagenomic contigs were predicted
515 by MetaGeneMark (version 3.26). CDS sequences of all samples were clustered by CD-HIT
516 (version 4.6.1)[89] to obtain unigenes with the following parameters: *-c 0.95 -aS 0.9 -d 0 -g 1 -M*
517 *20000 -T 20*. The CDS sequences from all samples are clustered together to group highly similar
518 or identical sequences, and a single representative sequence from each cluster is chosen as a
519 unigene. Unigene abundance for a certain sample were estimated by TPM based on the number
520 of aligned reads by bowtie2 (version 2.2.0)[90]. The TPM value for each Unigene was calculated by
521 dividing its RPK (Reads Per Kilobase) by the sum of RPK values across all Unigenes in the sample,
522 then multiplying the result by 1,000,000 to normalize expression levels to a per-million scale.
523 The figures in this study was widely plotted in R project ggplot2 package[91]. Top 10 phyla
524 were visualized in R with ggplot2 and ggalluvial as our previous publications[69,76]. Bray-Curtis
525 distance matrix was calculated in R with Vegan package[92] (version 2.5.7). NMDS was then
526 generated with Vegan and plotted with ggplot2 package. Adonis and anosim test were used to
527 calculate the significance of β diversity differences. The tree shape visualization of the taxonomic
528 diversity was performed by Metacoder package in R[93]. The functional annotations (GO, KEGG,
529 CARD, MGEs, VFDBs) of unigenes were obtained by aligning them against the NCBI NR database
530 (version 20191121) by DIAMOND (version 0.9.14)[94] with the following parameters: *-k 25 -e*
531 *0.00001 --query-cover 0 --min-score 0 --id 0 -p 20'*; *Command: srun -p all -c 20 singularity exec*
532 *--bind /public1/Programs,/public1/Softwares:/Softwares,/public*. Nitrogen cycling genes were
533 annotated with the NCycDB database[95]. Heatmaps were visualized with pheatmap package in R.
534 The functional deduction of bacteria enzyme functions (ECs) and metabolic pathway genes (KOs)
535 was performed by PICRUSt2[96].
536
537 **4.4. Microbial communities assembly analyses**
538 A dissimilarity-overlap curve (DOC) model was used to determine whether microbiota on
539 the red sandstone surface of the Leshan Giant Buddha have unique ecological dynamics in R with
540 DOC package (https://github.com/Russel88/DOC) according to previous reports[3,68,69]. The DOC
541 was obtained by plotting the dissimilarity (Jensen–Shannon divergence) against the overlap
542 fraction of taxa for each pairwise community[38] with 1000 bootstrap replicates to evaluate the
543 significance and initiation of negative slopes.
544 Null model analysis was performed as described by Stegen *et al.* [36,37] and visualized as
545 previous research[69]. The deviation of phylogenetic and taxonomic diversity was estimated with
546 999 randomizations. Beta mean nearest taxon distance (βMNTD) and beta nearest taxon index
547 (βNTI) were calculated with picante package in R[97]. Phylogenetic analysis were performed by
548 iqtree2 with 1000 bootstrap[98]. A significant deviation indicated the dominance of deterministic

549 processes, including homogeneous or heterogeneous selection processes when βNTI < −2 or
550 βNTI > 2, respectively. The Bray-Curtis based Raup-Crick (RCbray), the deviation between
551 Bray-Curtis and the null distribution, was then calculated to partition pairwise comparisons that
552 assigned the stochastic processes when |βNTI| < 2. The relative influence of homogenizing
553 dispersal and dispersal limitation was quantified as the fraction of pairwise comparisons with
554 RCbray < −0.95 and RCbray > 0.95, respectively. In addition, dispersal was seen as a stochastic
555 process in this research, not restricted to a deterministic or stochastic process as previously
556 described[3,18]. Low-occurrence ASVs with a prevalence less than 50% and low abundance ASVs
557 with total read counts lower than the number of samples were excluded to ensure the accuracy
558 in taxon-specific assembly characterization and reduce type I errors as presented in previous
559 research[3,69].
560
561 **4.5. Niche characteristics analysis**
562 Levins niche breadth index, Shannon niche breadth index, Schoener niche overlap index,
563 and Pianka niche overlap index were calculated with spaa package in R[99]. Generalists were
564 defined by ASVs with *Bcom* > 5, whereas specialists were defined by those with *Bcom* < 1.5[3,100].
565 Significance of the differences was tested by Wilcoxon signed-rank test.
566
567 **4.6. Network construction and topological feature analysis**
568 Microbial co-occurrence networks were constructed according to previous publication[101]
569 with modifications by ggClusterNet R package[102]. Topological features were also further visualized
570 with ggClusterNet in R. Spearman's correlation was applied to assess the relationships between
571 microbial taxa. Correlation coefficients with a threshold of r >= 0.6 and P values <= 0.05 were
572 retained for network construction to ensure significant and robust associations. The network was
573 further clustered using the *cluster_fast_greedy* algorithm, which identifies densely connected
574 sub-networks within the microbial community.
575
576 **4.7. Acknowledgements of English edition**
577 During the preparation of this work the authors used ChatGPT in order to check the English
578 grammar. After using this tool, the authors reviewed and edited the content as needed and take
579 full responsibility for the content of the publication.
580
581

582 ## Availability of data and materials

583 The raw sequence data reported in this paper have been deposited in the Genome
584 Sequence Archive in National Genomics Data Center, China National Center for Bioinformation /
585 Beijing Institute of Genomics, Chinese Academy of Sciences (GSA: CRA013382 & GSA: CRA013393)
586 that are publicly accessible at https://ngdc.cncb.ac.cn/gsa.
587 All scripts used in this study are publicly available at the GitHub repository
588 (https://github.com/Bowenw6/Microbiome_Buddha_Grotto_2023).
589

590 ## Author Contributions Statement

Bowen Wang: Conceptualization, Data curation, Formal analysis, Investigation, Methodology, Resources, Visualization, Writing - Original Draft, Writing - Review & Editing. **Chengshuai Zhu**: Conceptualization, Data curation, Investigation, Resources. **Xin Wang**: Conceptualization, Investigation, Resources. **Tianyu Yang**: Conceptualization, Investigation, Resources. **Bingjian Zhang**: Conceptualization, Funding acquisition, Supervision. **Yulan Hu**: Conceptualization, Funding acquisition, Project administration, Supervision, Writing - Review & Editing.

Competing interests

No, we declare that the authors have no competing interests, or other interests that might be perceived to influence the results and/or discussion reported in this paper.

Funding

This work is supported by the National Key Research and Development Program (2019YFC1520503)

Supplementary Files

Figure S1. The overall taxonomic community composition among all the samples.
Figure S2. Taxonomic community composition of the microbial communities in genus level.
Figure S3. Niche characterization of the stone surface microbial communities based on Shannon niche breadth index and Pianka niche overlap index.
Figure S4. Significant differences of metabolic pathway genes (KOs) among four groups.
Figure S5. Gene abundance within each nitrogen cycle pathway of the stone surface microbiota.
Table S1. Summaries for the details from the metagenome sequencing
Table S2. Relative abundances of dominant bacteria among 27 samples at the phylum level.
Table S3. Relative abundances of dominant bacteria among 27 samples at the genus level.
Table S4. Relative abundances of dominant fungi among 27 samples at the phylum level.
Table S5. Relative abundances of dominant fungi among 27 samples at the genus level.
Table S6. Habitat niche breadth of bacteria at the phylum level.
Table S7. Habitat niche breadth of fungi at the phylum level.
Table S8. Enzyme functions (ECs) among all samples.
Table S9. Metabolic pathway genes (KOs) among all samples.

References:

1 Liu, X. B., Koestler, R. J., Warscheid, T., Katayama, Y. & Gu, J. D. Microbial deterioration and sustainable conservation of stone monuments and buildings. *Nat Sustain* **3**, 991-1004 (2020). https://doi.org/10.1038/s41893-020-00602-5

2 Brewer, T. E. & Fierer, N. Tales from the tomb: the microbial ecology of exposed rock surfaces. *Environ Microbiol* **20**, 958-970 (2018). https://doi.org/10.1111/1462-2920.14024

3 He, J. *et al.* From surviving to thriving, the assembly processes of microbial communities in stone biodeterioration: A case study of the West Lake UNESCO World Heritage area in China. *Sci Total Environ* **805**, 150395 (2022). https://doi.org/10.1016/j.scitotenv.2021.150395

4 Qiang, L., Zhang, B. B., Yang, B. X. & Ged, C. Q. Deterioration-Associated Microbiome of Stone Monuments: Structure, Variation, and Assembly. *Appl Environ Microbiol* **84**, e02680-02617-02617 (2018).

5 Li, T., Hu, Y. & Zhang, B. Biomineralization Induced by Colletotrichum acutatum: A Potential Strategy for Cultural Relic Bioprotection. *Front Microbiol* **9**, 1884 (2018).

6 Jroundi, F., Gonzalez-Muñoz, M. T. & Rodriguez-Navarro, C. in *Microorganisms in the Deterioration and Preservation of Cultural Heritage* (ed Edith Joseph) 281-299 (Springer International Publishing, 2021).

7 Liu, X. *et al.* Biofilms on stone monuments: biodeterioration or bioprotection? *Trends Microbiol* **30**, 816-819 (2022). https://doi.org/https://doi.org/10.1016/j.tim.2022.05.012

8 Li, J. *et al.* The active microbes and biochemical processes contributing to deterioration of Angkor sandstone monuments under the tropical climate in Cambodia – A review. *J Cult Herit* **47**, 218-226 (2021). https://doi.org/https://doi.org/10.1016/j.culher.2020.10.010

9 Ding, X. *et al.* Microbiome and nitrate removal processes by microorganisms on the ancient Preah Vihear temple of Cambodia revealed by metagenomics and N-15 isotope analyses. *Appl Microbiol Biotechnol* **104**, 9823-9837 (2020). https://doi.org/10.1007/s00253-020-10886-4

10 Wu, F. *et al.* Metagenomic and metaproteomic insights into the microbiome and the key geobiochemical potentials on the sandstone of rock-hewn Beishiku Temple in Northwest China. *Sci Total Environ* **893**, 164616 (2023). https://doi.org/https://doi.org/10.1016/j.scitotenv.2023.164616

11 Fidanza, M. R. & Caneva, G. Natural biocides for the conservation of stone cultural heritage: A review. *J Cult Herit* **38**, 271-286 (2019). https://doi.org/https://doi.org/10.1016/j.culher.2019.01.005

12 Li, Q., Wu, C., He, J. & Zhang, B. Unraveling the microbiotas and key genetic contexts identified on stone heritage using illumina and nanopore sequencing platforms. *Int Biodeter Biodegr* **185**, 105688 (2023). https://doi.org/https://doi.org/10.1016/j.ibiod.2023.105688

13 Ding, X. *et al.* Microbiome characteristics and the key biochemical reactions identified on stone world cultural heritage under different climate conditions. *Journal of Environmental Management* **302**, 114041 (2022). https://doi.org/https://doi.org/10.1016/j.jenvman.2021.114041

14 Ennis, N. J., Dharumaduri, D., Bryce, J. G. & Tisa, L. S. Metagenome Across a Geochemical Gradient of Indian Stone Ruins Found at Historic Sites in Tamil Nadu, India. *Microb Ecol* **81**, 385-395 (2021). https://doi.org/10.1007/s00248-020-01598-3

15 Louati, M. *et al.* Elucidating the ecological networks in stone-dwelling microbiomes. *Environ Microbiol* **22**, 1467-1480 (2020). https://doi.org/https://doi.org/10.1111/1462-2920.14700

16 Li, T., Cai, Y. & Ma, Q. Microbial Diversity on the Surface of Historical Monuments in Lingyan Temple, Jinan, China. *Microb Ecol* (2022). https://doi.org/10.1007/s00248-021-01955-w

17 Cattò, C. *et al.* Biofilm colonization of stone materials from an Australian outdoor sculpture:

Importance of geometry and exposure. *Journal of Environmental Management* **339**, 117948 (2023). https://doi.org/https://doi.org/10.1016/j.jenvman.2023.117948

18 Zhou, J. & Ning, D. Stochastic Community Assembly: Does It Matter in Microbial Ecology? *MMBR* **81**, e00002-00017 (2017). https://doi.org/10.1128/MMBR.00002-17

19 Dal Bello, M., Lee, H., Goyal, A. & Gore, J. Resource–diversity relationships in bacterial communities reflect the network structure of microbial metabolism. *Nature Ecology & Evolution* **5**, 1424-1434 (2021). https://doi.org/10.1038/s41559-021-01535-8

20 Goldford, J. E. *et al.* Emergent simplicity in microbial community assembly. *Science* **361**, 469-474 (2018). https://doi.org/10.1126/science.aat1168

21 Ning, D. *et al.* A quantitative framework reveals ecological drivers of grassland microbial community assembly in response to warming. *Nat Commun* **11**, 4717 (2020). https://doi.org/10.1038/s41467-020-18560-z

22 Chase, J. M. Stochastic Community Assembly Causes Higher Biodiversity in More Productive Environments. *Science* **328**, 1388-1391 (2010). https://doi.org/10.1126/science.1187820

23 Ofițeru, I. D. *et al.* Combined niche and neutral effects in a microbial wastewater treatment community. *PNAS* **107**, 15345-15350 (2010). https://doi.org/10.1073/pnas.1000604107

24 Chesson, P. Mechanisms of Maintenance of Species Diversity. *Annual Review of Ecology, Evolution, and Systematics* **31**, 343-366 (2000). https://doi.org/https://doi.org/10.1146/annurev.ecolsys.31.1.343

25 Fargione, J., Brown, C. S. & Tilman, D. Community assembly and invasion: An experimental test of neutral versus niche processes. *PNAS* **100**, 8916-8920 (2003). https://doi.org/10.1073/pnas.1033107100

26 Chave, J. Neutral theory and community ecology. *Ecol Lett* **7**, 241-253 (2004). https://doi.org/https://doi.org/10.1111/j.1461-0248.2003.00566.x

27 Vega, N. M. & Gore, J. Stochastic assembly produces heterogeneous communities in the Caenorhabditis elegans intestine. *PLOS Biology* **15**, e2000633 (2017). https://doi.org/10.1371/journal.pbio.2000633

28 Ning, D. *et al.* Environmental stress mediates groundwater microbial community assembly. *Nature Microbiology* **9**, 490-501 (2024). https://doi.org/10.1038/s41564-023-01573-x

29 He, Q. *et al.* Temperature and microbial interactions drive the deterministic assembly processes in sediments of hot springs. *Sci Total Environ* **772**, 145465 (2021). https://doi.org/https://doi.org/10.1016/j.scitotenv.2021.145465

30 Tolkkinen, M. *et al.* Multi-stressor impacts on fungal diversity and ecosystem functions in streams: natural vs. anthropogenic stress. *Ecology* **96**, 672-683 (2015). https://doi.org/https://doi.org/10.1890/14-0743.1

31 Huot, O. B. & Tamborindeguy, C. Drought stress affects olanum lycopersicum susceptibility to actericera cockerelli colonization. *Entomologia Experimentalis et Applicata* **165**, 70-82 (2017). https://doi.org/https://doi.org/10.1111/eea.12627

32 Luo, C., Lü, F., Shao, L. & He, P. Application of eco-compatible biochar in anaerobic digestion to relieve acid stress and promote the selective colonization of functional microbes. *Water Res* **68**, 710-718 (2015). https://doi.org/https://doi.org/10.1016/j.watres.2014.10.052

33 Bai, F. *et al.* Microbial biofilms on a giant monolithic statue of Buddha: The symbiosis of microorganisms and mosses and implications for bioweathering. *Int Biodeter Biodegr* **156** (2021). https://doi.org/ARTN 105106 10.1016/j.ibiod.2020.105106

34 Zhu, C. *et al.* Analysis of the Microbiomes on Two Cultural Heritage Sites. *Geomicrobiol J,* 1-10 (2022). https://doi.org/10.1080/01490451.2022.2137604

35 Zhu, C. *et al.* Unveiling the dual role of biocolonization: a case study on the deterioration and preservation of sandstone monuments in Leshan Giant Buddha, China. *World Journal of Microbiology and Biotechnology* **41**, 25 (2025). https://doi.org/10.1007/s11274-024-04237-y

36 Stegen, J. C., Lin, X., Konopka, A. E. & Fredrickson, J. K. Stochastic and deterministic assembly processes in subsurface microbial communities. *ISME J* **6**, 1653-1664 (2012). https://doi.org/10.1038/ismej.2012.22

37 Stegen, J. C. *et al.* Quantifying community assembly processes and identifying features that impose them. *ISME J* **7**, 2069-2079 (2013). https://doi.org/10.1038/ismej.2013.93

38 Bashan, A. *et al.* Universality of human microbial dynamics. *Nature* **534**, 259-262 (2016). https://doi.org/10.1038/nature18301

39 Levins, R. *Evolution in Changing Environments Some Theoretical Explorations. (MPB-2)*. (Princeton University Press, 1968).

40 Sexton, J. P., Montiel, J., Shay, J. E., Stephens, M. R. & Slatyer, R. A. Evolution of Ecological Niche Breadth. *Annual Review of Ecology, Evolution, and Systematics* **48**, 183-206 (2017). https://doi.org/10.1146/annurev-ecolsys-110316-023003

41 von Meijenfeldt, F. A. B., Hogeweg, P. & Dutilh, B. E. A social niche breadth score reveals niche range strategies of generalists and specialists. *Nature Ecology & Evolution* **7**, 768-781 (2023). https://doi.org/10.1038/s41559-023-02027-7

42 Meng, H., Zhang, X., Katayama, Y., Ge, Q. & Gu, J.-D. Microbial diversity and composition of the Preah Vihear temple in Cambodia by high-throughput sequencing based on genomic DNA and RNA. *Int Biodeter Biodegr* **149** (2020).

43 Meng, S. *et al.* Community structures and biodeterioration processes of epilithic biofilms imply the significance of micro-environments. *Sci Total Environ* **876**, 162665 (2023). https://doi.org/https://doi.org/10.1016/j.scitotenv.2023.162665

44 Chen, X. *et al.* The Organisms on Rock Cultural Heritages: Growth and Weathering. *Geoheritage* **13** (2021). https://doi.org/ARTN 5610.1007/s12371-021-00588-2

45 Escalas, A. *et al.* Microbial functional diversity: From concepts to applications. *Ecology and Evolution* **9**, 12000-12016 (2019). https://doi.org/https://doi.org/10.1002/ece3.5670

46 Prosser, J. I. *et al.* The role of ecological theory in microbial ecology. *Nat Rev Microbiol* **5**, 384-392 (2007). https://doi.org/10.1038/nrmicro1643

47 Sterflinger, K. *et al.* Future directions and challenges in biodeterioration research on historic materials and cultural properties. *Int Biodeter Biodegr* **129**, 10-12 (2018). https://doi.org/https://doi.org/10.1016/j.ibiod.2017.12.007

48 Wu, Y. *et al.* Monitoring the Deterioration of Masonry Relics at a UNESCO World Heritage Site. *KSCE Journal of Civil Engineering* **25**, 3097-3106 (2021). https://doi.org/10.1007/s12205-021-1716-z

49 Zhang, X. W., Ge, Q. Y., Zhu, Z. B., Deng, Y. M. & Gu, J. D. Microbiological community of the Royal Palace in Angkor Thom and Beng Mealea of Cambodia by Illumina sequencing based on 16S rRNA gene. *Int Biodeter Biodegr* **134**, 127-135 (2018). https://doi.org/10.1016/j.ibiod.2018.06.018

50 Schröer, L., De Kock, T., Cnudde, V. & Boon, N. Differential colonization of microbial communities inhabiting Lede stone in the urban and rural environment. *Sci Total Environ* **733**,

764 139339 (2020). https://doi.org/https://doi.org/10.1016/j.scitotenv.2020.139339
765 51 Qian, Y., Liu, X., Hu, P., Gao, L. & Gu, J.-D. Identifying the major metabolic potentials of
766 microbial-driven carbon, nitrogen and sulfur cycling on stone cultural heritage worldwide. *Sci*
767 *Total Environ* **954**, 176757 (2024).
768 https://doi.org/https://doi.org/10.1016/j.scitotenv.2024.176757
769 52 Grossi, C. E. M. *et al.* Methylobacterium sp. 2A Is a Plant Growth-Promoting Rhizobacteria
770 That Has the Potential to Improve Potato Crop Yield Under Adverse Conditions. *Frontiers in*
771 *Plant Science* **11** (2020). https://doi.org/10.3389/fpls.2020.00071
772 53 Ramond, P., Galand, P. E. & Logares, R. Microbial functional diversity and redundancy: moving
773 forward. *FEMS Microbiology Reviews* **49**, fuae031 (2025).
774 https://doi.org/10.1093/femsre/fuae031
775 54 Tian, L. *et al*. Deciphering functional redundancy in the human microbiome. *Nat Commun* **11**,
776 6217 (2020). https://doi.org/10.1038/s41467-020-19940-1
777 55 Li, H. *et al.* Food provisioning results in functional, but not compositional, convergence of the
778 gut microbiomes of two wild Rhinopithecus species: Evidence of functional redundancy in the
779 gut microbiome. *Sci Total Environ* **858**, 159957 (2023).
780 https://doi.org/https://doi.org/10.1016/j.scitotenv.2022.159957
781 56 Moya, A. & Ferrer, M. Functional Redundancy-Induced Stability of Gut Microbiota Subjected
782 to Disturbance. *Trends Microbiol* **24**, 402-413 (2016).
783 https://doi.org/10.1016/j.tim.2016.02.002
784 57 Tian, L. & Zhang, J. Dynamics of Rabies Epidemics in Vampire Bats. *Complexity* **2020**, 7032451
785 (2020). https://doi.org/https://doi.org/10.1155/2020/7032451
786 58 Talbot, J. M. *et al.* Endemism and functional convergence across the North American soil
787 mycobiome. *PNAS* **111**, 6341-6346 (2014). https://doi.org/10.1073/pnas.1402584111
788 59 Zeng, Q. *et al.* Stable functional structure despite high taxonomic variability across fungal
789 communities in soils of old-growth montane forests. *Microbiome* **11**, 217 (2023).
790 https://doi.org/10.1186/s40168-023-01650-7
791 60 Chen, H. *et al.* Functional Redundancy in Soil Microbial Community Based on Metagenomics
792 Across the Globe. *Front Microbiol* **13** (2022).
793 61 Zhou, J. *et al.* The diversity and ecological significance of microbial traits potentially involved
794 in B12 biosynthesis in the global ocean. *mLife* **2**, 416-427 (2023).
795 https://doi.org/https://doi.org/10.1002/mlf2.12095
796 62 Burke, C., Steinberg, P., Rusch, D., Kjelleberg, S. & Thomas, T. Bacterial community assembly
797 based on functional genes rather than species. *PNAS* **108**, 14288-14293 (2011).
798 https://doi.org/10.1073/pnas.1101591108
799 63 Louca, S. *et al.* Function and functional redundancy in microbial systems. *Nature Ecology &*
800 *Evolution* **2**, 936-943 (2018). https://doi.org/10.1038/s41559-018-0519-1
801 64 Chikina, M., Robinson, J. D. & Clark, N. L. Hundreds of Genes Experienced Convergent Shifts in
802 Selective Pressure in Marine Mammals. *Molecular Biology and Evolution* **33**, 2182-2192
803 (2016). https://doi.org/10.1093/molbev/msw112
804 65 Winemiller, K. O., Fitzgerald, D. B., Bower, L. M. & Pianka, E. R. Functional traits, convergent
805 evolution, and periodic tables of niches. *Ecol Lett* **18**, 737-751 (2015).
806 https://doi.org/https://doi.org/10.1111/ele.12462
807 66 Nie, Y. *et al.* Species Divergence vs. Functional Convergence Characterizes Crude Oil Microbial

Community Assembly. *Front Microbiol* **7** (2016).

67 Li, P. *et al.* Global diversity and biogeography of potential phytopathogenic fungi in a changing world. *Nat Commun* **14**, 6482 (2023). https://doi.org/10.1038/s41467-023-42142-4

68 Gao, C. *et al.* Fungal community assembly in drought-stressed sorghum shows stochasticity, selection, and universal ecological dynamics. *Nat Commun* **11**, 34 (2020). https://doi.org/10.1038/s41467-019-13913-9

69 Wang, B., Zhu, C., Hu, Y., Zhang, B. & Wang, J. Dynamics of microbial community composition during degradation of silks in burial environment. *Sci Total Environ* **883**, 163694 (2023). https://doi.org/https://doi.org/10.1016/j.scitotenv.2023.163694

70 Meng, H., Luo, L., Chan, H. W., Katayama, Y. & Gu, J.-D. Higher diversity and abundance of ammonia-oxidizing archaea than bacteria detected at the Bayon Temple of Angkor Thom in Cambodia. *Int Biodeter Biodegr* **115**, 234-243 (2016). https://doi.org/https://doi.org/10.1016/j.ibiod.2016.08.021

71 Puente-Sánchez, F., Pascual-García, A., Bastolla, U., Pedrós-Alió, C. & Tamames, J. Cross-biome microbial networks reveal functional redundancy and suggest genome reduction through functional complementarity. *Communications Biology* **7**, 1046 (2024). https://doi.org/10.1038/s42003-024-06616-5

72 MacArthur, R. Species packing and competitive equilibrium for many species. *Theoretical Population Biology* **1**, 1-11 (1970). https://doi.org/https://doi.org/10.1016/0040-5809(70)90039-0

73 Advani, M., Bunin, G. & Mehta, P. Statistical physics of community ecology: a cavity solution to MacArthur's consumer resource model. *Journal of Statistical Mechanics: Theory and Experiment* **2018**, 033406 (2018). https://doi.org/10.1088/1742-5468/aab04e

74 Marsland, R., III *et al.* Available energy fluxes drive a transition in the diversity, stability, and functional structure of microbial communities. *PLOS Computational Biology* **15**, e1006793 (2019). https://doi.org/10.1371/journal.pcbi.1006793

75 Sriswasdi, S., Yang, C.-c. & Iwasaki, W. Generalist species drive microbial dispersion and evolution. *Nat Commun* **8**, 1162 (2017). https://doi.org/10.1038/s41467-017-01265-1

76 Wang, B., Qi, M., Ma, Y., Zhang, B. & Hu, Y. Microbiome Diversity and Cellulose Decomposition Processes by Microorganisms on the Ancient Wooden Seawall of Qiantang River of Hangzhou, China. *Microb Ecol* **86**, 2109-2119 (2023). https://doi.org/10.1007/s00248-023-02221-x

77 Wang, B., Zhu, C., Wang, B., Zhang, B. & Hu, Y. Analysis of the biocorrosion community from ancient wooden constructions at Tianluoshan (7000–6300 cal BP), Zhejiang Province, China. *Heritage Science* **12**, 189 (2024). https://doi.org/10.1186/s40494-024-01304-3

78 Zhu, C. *et al.* Application and evaluation of a new blend of biocides for biological control on cultural heritages. *Int Biodeter Biodegr* **178**, 105569 (2023). https://doi.org/https://doi.org/10.1016/j.ibiod.2023.105569

79 Li, J. *et al.* Changes in soil microbial communities at Jinsha earthen site are associated with earthen site deterioration. *BMC Microbiology* **20**, 147 (2020). https://doi.org/10.1186/s12866-020-01836-1

80 Wang, X., Wang, B., Hu, Y., Zhang, Z. & Zhang, B. Activity-based protein profiling technology reveals malate dehydrogenase as the target protein of cinnamaldehyde against Aspergillus niger. *Int J Food Microbiol* **417**, 110685 (2024).

852 https://doi.org/https://doi.org/10.1016/j.ijfoodmicro.2024.110685
853 81 Logue, J. B. *et al.* Experimental insights into the importance of aquatic bacterial community
854 composition to the degradation of dissolved organic matter. *ISME J* **10**, 533-545 (2016).
855 https://doi.org/10.1038/ismej.2015.131
856 82 Chen, T. *et al.* The Genome Sequence Archive Family: Toward Explosive Data Growth and
857 Diverse Data Types. *Genomics, Proteomics & Bioinformatics* **19**, 578-583 (2021).
858 https://doi.org/https://doi.org/10.1016/j.gpb.2021.08.001
859 83 Members, C.-N. & Partners. Database Resources of the National Genomics Data Center, China
860 National Center for Bioinformation in 2022. *Nucleic Acids Research* **50**, D27-D38 (2022).
861 https://doi.org/10.1093/nar/gkab951
862 84 Callahan, B. J. *et al.* DADA2: High-resolution sample inference from Illumina amplicon data.
863 *Nat Methods* **13**, 581-583 (2016). https://doi.org/10.1038/nmeth.3869
864 85 Bolyen, E. *et al.* Reproducible, interactive, scalable and extensible microbiome data science
865 using QIIME 2. *Nat Biotechnol* **37**, 852-857 (2019).
866 https://doi.org/10.1038/s41587-019-0209-9
867 86 Wang, Q., Garrity, G. M., Tiedje, J. M. & Cole, J. R. Nave Bayesian Classifier for Rapid
868 Assignment of rRNA Sequences into the New Bacterial Taxonomy. *Appl Environ Microbiol* **73**,
869 5261 (2007).
870 87 Pruesse, E. *et al.* SILVA: a comprehensive online resource for quality checked and aligned
871 ribosomal RNA sequence data compatible with ARB. *Nucleic Acids Res* **35**, 7188-7196 (2007).
872 https://doi.org/10.1093/nar/gkm864
873 88 Nilsson, R. H. *et al.* The UNITE database for molecular identification of fungi: handling dark
874 taxa and parallel taxonomic classifications. *Nucleic Acids Research* **47**, D259-D264 (2019).
875 https://doi.org/10.1093/nar/gky1022
876 89 Fu, L., Niu, B., Zhu, Z., Wu, S. & Li, W. CD-HIT: accelerated for clustering the next-generation
877 sequencing data. *Bioinformatics* **28**, 3150-3152 (2012).
878 https://doi.org/10.1093/bioinformatics/bts565
879 90 Langmead, B. & Salzberg, S. L. Fast gapped-read alignment with Bowtie 2. *Nat Methods* **9**,
880 357-359 (2012). https://doi.org/10.1038/nmeth.1923
881 91 Wickham, H. ggplot2. *WIREs Computational Statistics* **3**, 180-185 (2011).
882 https://doi.org/https://doi.org/10.1002/wics.147
883 92 Dixon, P. VEGAN, a package of R functions for community ecology. *Journal of Vegetation*
884 *Science* **14**, 927-930 (2003).
885 https://doi.org/https://doi.org/10.1111/j.1654-1103.2003.tb02228.x
886 93 Foster, Z. S. L., Sharpton, T. J. & Grünwald, N. J. Metacoder: An R package for visualization and
887 manipulation of community taxonomic diversity data. *PLOS Computational Biology* **13**,
888 e1005404 (2017). https://doi.org/10.1371/journal.pcbi.1005404
889 94 Buchfink, B., Xie, C. & Huson, D. H. Fast and sensitive protein alignment using DIAMOND. *Nat*
890 *Methods* **12**, 59-60 (2015). https://doi.org/10.1038/nmeth.3176
891 95 Tu, Q., Lin, L., Cheng, L., Deng, Y. & He, Z. NCycDB: a curated integrative database for fast and
892 accurate metagenomic profiling of nitrogen cycling genes. *Bioinformatics* **35**, 1040-1048
893 (2019). https://doi.org/10.1093/bioinformatics/bty741
894 96 Douglas, G. M. *et al.* PICRUSt2 for prediction of metagenome functions. *Nat Biotechnol* **38**,
895 685-688 (2020). https://doi.org/10.1038/s41587-020-0548-6

896 97 Kembel, S. W. *et al.* Picante: R tools for integrating phylogenies and ecology. *Bioinformatics* **26**,
897 1463-1464 (2010). https://doi.org/10.1093/bioinformatics/btq166
898 98 Nguyen, L.-T., Schmidt, H. A., von Haeseler, A. & Minh, B. Q. IQ-TREE: A Fast and Effective
899 Stochastic Algorithm for Estimating Maximum-Likelihood Phylogenies. *Molecular Biology and*
900 *Evolution* **32**, 268-274 (2015). https://doi.org/10.1093/molbev/msu300
901 99 Zhang, J. M., KP. spaa: An R package for computing species association and niche overlap. .
902 *Research Progress of Biodiversity Conservation in China (in Chinese)* **X**, 165-174 (2014).
903 100 Pandit, S. N., Kolasa, J. & Cottenie, K. Contrasts between habitat generalists and specialists:
904 an empirical extension to the basic metacommunity framework. *Ecology* **90**, 2253-2262
905 (2009). https://doi.org/https://doi.org/10.1890/08-0851.1
906 101 Hao, X. *et al.* Effects on community composition and function Pinus massoniana infected by
907 Bursaphelenchus xylophilus. *BMC Microbiology* **22**, 157 (2022).
908 https://doi.org/10.1186/s12866-022-02569-z
909 102 Wen, T. *et al.* ggClusterNet: An R package for microbiome network analysis and
910 modularity-based multiple network layouts. *iMeta* **1**, e32 (2022).
911 https://doi.org/https://doi.org/10.1002/imt2.32
912